Performance modelling of zeolite-based potentiometric sensors

Martin Jendrlin [a], Aleksandar Radu [a,*], Vladimir Zholobenko [a,*], Dmitry Kirsanov [b,*]

[a] Lennard-Jones Laboratories, Keele University, Keele, Staffordshire ST5 5BG, United Kingdom
[b] Institute of Chemistry, Mendeleev Center, St. Petersburg State University, Universitetskaya nab. 7/9, Russian Federation

A B S T R A C T

Developing simple and cost-effective electrochemical sensors for widespread on-site application is of considerable practical importance in agriculture, environmental monitoring and food science. Among multiple sensing platforms, potentiometry is particularly effective in terms of simplicity, low cost and mass-production. This work is focused on a systematic analysis of the structure – performance relationship using chemometric techniques, which can be applied to sensor arrays with varying response patterns. The potentiometric sensitivity of zeolite-modified electrodes, containing thirteen synthetic and three natural zeolites, in aqueous solutions of Na^+, K^+, NH_4^+, Ca^{2+} and Mg^{2+} has been correlated with a range of zeolite characteristics using PCA and PLS modelling, thus demonstrating how structural and physical properties impact the performance of zeolite-modified potentiometric sensors. In addition to steric factors, e.g. zeolite pore size, the important characteristics governing the sensor performance are the Si/Al ratio and the presence of specific extraframework cations. For instance, K^+ and Na^+ show a strong effect on the potentiometric sensitivity towards Ca^{2+}. The level of precision achieved by the PLS models indicates that semi-quantitative predictions are feasible. To improve the computational models, larger sets of data with a wider range of zeolite-modified sensors are necessary. The constituent materials of such sensors should have a set of well-defined properties, which can be controlled and tuned for a particular application. It is anticipated that synthetic rather than natural zeolites would satisfy such requirements.

1. Introduction

Zeolites are crystalline microporous aluminosilicates. Their uniform porosity, thermal stability, non-swelling in water, ion-exchange capacity and structural diversity make them suitable for a wide range of commercial applications. They are established as core materials in industrial catalysis and water treatment facilities, but zeolites can also be utilised as sensor components, serving either as matrices for other active constituents or as functional sensing elements that are of considerable interest in zeolite science [1]. As sensing components, zeolites could be applied for the detection of gaseous substances [2–6] or as electrochemical sensors of dissolved species [7–10]. In the latter group, which is a subgroup of chemically modified electrodes, zeolites are utilised in zeolite-modified electrodes (ZME) [11]. Since zeolites are electrical insulators, they have to be in contact with a conductive matrix in order to be used as sensing electrode components. Among the reported zeolite-containing electrodes, two main groups can be distinguished: zeolite - conductive polymer membranes [12–16] and zeolite - graphite matrices, among which the zeolite - modified carbon paste electrodes [17–19] are the most common.

In the electrochemical characterisation of various species, voltammetric, amperometric, conductometric and potentiometric techniques have been used [7–10]. Among these techniques, potentiometry, although a very simple method, is rather infrequently used for the detection of cationic species. Interestingly, the first reports on zeolites utilised as electrode components [16,20] were potentiometry-based.

According to the literature data [7–10], zeolites can, to a certain degree, selectively detect a variety of species: cationic dyes [21], detergents [15], pesticides and fungicides [22], neurotransmitters and vitamins [12,23], amino acids [24,25] and inorganic cations [26–28] (see Table 1). The potentiometric selectivity values presented in Table 1 were either calculated by separate solution method or, if not explicitly stated, they were determined from the reported responses of electrodes to specific species. However, the selectivity of zeolites is relatively poor compared to classical ionophore-based electrodes. This fact has probably discouraged a wider use of ZMEs, therefore, a limited amount of research has been conducted on elucidating the detection mechanisms and the parameters affecting the potentiometric response of ZME.

* Corresponding authors.
E-mail addresses: a.radu@keele.ac.uk (A. Radu), v.l.zholobenko@keele.ac.uk (V. Zholobenko), d.kirsanov@gmail.com (D. Kirsanov).

Zeolites with adsorbed cationic exchangers [29,30] should be mentioned as a separate category since these components are not confined within the zeolite, but rather are deposited on its external surface. Therefore, zeolites serve only as immobilisation matrices rather than as electroactive components. The observed selectivity in this group of sensors has been mainly following the Hoffmeister series of anions.

Most of the reported work is confined to the use of zeolites with the faujasite (FAU) framework, such as NaX and NaY [15,31,32], with several other framework types described less frequently. Additionally, reports are also focused on the detection performance rather than on elucidating the detection mechanism and the structure - function relationship. An attempt to relate the electrochemical responses to the chemical and physical parameters of the analytes and zeolites have been reported for cyclic voltammetry [26,33] and indirect amperometry techniques [34], only. The steric factors (cation diameter, zeolite pore size) and charge separation have been stated as the limiting factors of the ZME performance. Even though some interesting insight has been provided, only a limited number of zeolites frameworks has been used, thus not covering a wider range of zeolite features available [26,33,34]. Moreover, the studied parameters have been targeted more on the optimisation of the specific electrochemical technique, so the conclusions provided may not be applied completely to potentiometric applications.

In this work, the observed electrochemical responses of zeolite-containing electrodes to mono- (K^+, NH_4^+, Na^+) and divalent (Ca^{2+}, Mg^{2+}) cations are determined by potentiometric studies and systematically analysed using chemometric techniques. Such an approach is essential for the rational design of ZME, particularly in the case of multi-sensor arrays. Indeed, such systems with varying response patterns can significantly improve the selectivity of the zeolite-based sensors [35]. However, to the best of our knowledge, this is the first comprehensive investigation relating zeolite properties (Si/Al ratio, pore size, etc) to their performance as the materials for potentiometric sensing. Our work demonstrates that the performance of zeolite-containing electrodes can be rationalised based on the system parameters and that predictive models can be developed using statistical approaches.

2. Experimental section

Graphite powder (particle size <20 μm, synthetic), sodium chloride (NaCl), potassium chloride (KCl), ammonium chloride (NH_4Cl), calcium chloride ($CaCl_2$), magnesium chloride ($MgCl_2$) and zinc chloride ($ZnCl_2$) were purchased from Sigma-Aldrich. Zeolites NaX (Si/Al=1.3), KX (Si/Al=1.3), NaY (Si/Al=2.6) and KY (Si/Al=2.6) were purchased from

Table 1
A summary of the literature data on ZME potentiometric studies.

Species of interest	Observed selectivity	LOD (M)	Linear range (M)	Zeolite used	Preparation method	Ref.
Na^+	Na^+>>TEA^+ [a]		0.7 – 2	NaA	Epoxy resin membrane	[16]
K^+	Cs^+> Rb^+> K^+> Na^+> Li^+	1×10^{-5} 2×10^{-5} 2.5×10^{-5} 4×10^{-5}	10^{-4} – 0.1	CaA	Low−viscosity epoxy resin membrane	[13]
Cs^+	Cs^+> Ag^+, K^+> Na^+> Li^+ Cs^+>>Ba^{2+}> Ca^{2+}> Cu^{2+}	2×10^{-5}	3×10^{-5} – 0.1	MOR	Epoxy resin membrane	[14]
Cd^{2+}	Cd^{2+}> Al^{3+}	–	1×10^{-5} – 1×10^{-2}	NaA	Polysulfone coated zeolite on glassy carbon	[36]
Cs^+	Cs^+> K^+> Na^+> Li^+	3×10^{-5}	5×10^{-4} – 0.1	NaX	Polydimethoxysilane membrane on Ir disks	[15]
HDPCL	HDPCL>DTACL[b]	–	–	NaA	Polydimethoxysilane membrane on Ir disks	[15]
K^+	K^+> Ca^{2+}> Ba^{2+}>Li^+	–	–	CHA	Neat-pressed zeolite disk	[20]
H^+	H^+>>Li^+> Na^+> NH_4^+> K^+> Fe^{2+}> Ca^{2+}	1×10^{-12}	1×10^{-12} – 0.1	"Natural zeolite" (Si/Al= 5.5)	Screen−printed sol−gel graphite mix	[37]
K^+	K^+>>Na^+	1×10^{-6}	1×10^{-6} – 1×10^{-2}	ZSM-5	Polypyrrole/zeolite composite	[38]
Cd^{2+}	Pb^{2+}> Cd^{2+}	–	1×10^{-6} – 1.5×10^{-2}	NaY	TEOS "healed" zeolite membrane[c]	[39]
NH_4^+	NH_4^+>>K^+, Na^+, H^+	1×10^{-8}	1×10^{-7} – 1×10^{-4}	Clinoptilolite	Siloprene−zeolite membrane (ISFET)[d]	[40]
Urea	NH_4^+>>K^+, Na^+, H^+ Urea>Hg^{2+}, Cu^{2+}, Ag^+	3×10^{-5}	3×10^{-5} – 5×10^{-3}	Clinoptilolite	Siloprene−zeolite−urease membrane (ISFET, ENFET)[e]	[41]
Cs^+, Na^+	Na^+> Cs^+	–	–	NaY, NaA, MOR	Neat-pressed zeolite disks	[42]
Cs^+	Cs^+> K^+> NH_4^+> Na^+> Ca^{2+}> Cd^{2+}> Pb^{2+}> Mg^{2+}> Cu^{2+}> Li^+> Ni^{2+}	4×10^{-5}	1×10^{-4} – 0.1	KY	PTEV[f] (benzyl acetate), silicone oil	[43]
Thionine	Thionine>RB6G>RB[g]> Na^+> NH_4^+> MB[g]>> Sr^{2+}>>Ca^{2+}> Zn^{2+}> Ni^{2+}> Co^{2+}> Al^{3+}> Mn^{2+}> Fe^{2+}	8×10^{-7}	1×10^{-6} – 1×10^{-2}	MOR (ion-exchanged by thionine)	PVC (DBP)[h] membrane	[21]
Cs^+	Cs^+> Tl^+> Cr^{2+}> NH_4^+, Na^+> Cu^{2+}, Li^+, Al^{3+}> Mg^{2+}> Bi^{2+}> Ca^{2+}> Ba^{2+}, Mn^{2+}, Cd^{2+}> Zn^{2+}, Co^{2+}> Ni^{2+}	7.3×10^{-6}	1×10^{-5} – 0.1	KY	Sol−gel matrix	[44]
Cs^+	Cs^+> NH_4^+> Pb^{2+}> Zn^{2+}> Cd^{2+}> Ca^{2+}> Ni^{2+}> Hg^{2+}> Mg^{2+}	5.2×10^{-5}	1.0×10^{-4} – 0.1	KY	PVC (DBP)	[45]

[a] TEA^+ - tetraethylammonium cation
[b] HDPCL - hexadecylpyridinium chloride, DTACL - Dodecyltrimethylammonium chloride (cationic detergents)
[c] TEOS - tetraethylorthosilicate
[d] ISFET - ion-selective field-effect transistor
[e] ENFET - enzyme-linked field-effect transistor
[f] PTEV - poly(tetrafluoroethylene-co-ethylene-co-vinyl acetate)
[g] RB6G - rhodamine B6G, RB - rhodamine B, MB - methylene blue (all mentioned compounds including thionine are cationic dyes)
[h] DBP - dibutyl phthalate.

Riogen, USA. Zeolites MAP (Si/Al=1.0), NaA (Si/Al=1.0) and KA (Si/Al=1.0) were provided by Crosfield, zeolites MOR (Si/Al=10.0), FER (Si/Al=10.0), BEA-12 (Si/Al=12.5), BEA-19 (Si/Al=19.0) and ZSM-5 (Si/Al=40.0) were obtained from Zeolyst, and zeolite LTL (Si/Al=3.1) was supplied by Tosoh, Japan. Zeolites HEU-A and HEU-B were from Zeodex, UK, HEU-C was provided by Prof A. Walcarius (Université de Lorraine, France). OHP universal film (clear 4243–100 μm) from Q-connect was used as a substrate. All the standard aqueous solutions were prepared with ultrapure water obtained using a Pico Pure 3 system.

2.1. Zeolite characterisation

Zeolites were characterised by powder X-ray diffraction (using a Bruker D8 Advance diffractometer Cu Kα at 40 kV and 40 mA, 2θ=5 −60°), scanning electron microscopy (Hitachi TM 3000 with Bruker EDX system at 500x magnification, 300 s EDX data collection time) and FTIR spectroscopy (using Thermo iS10 spectrometer with a custom-made cell, 6000 −1000 cm^{-1}, 64 scans, 4 cm^{-1} resolution, transmission mode) Further details are provided in Ref 46,47 and in Supplementary Information.

2.2. Ion-sensitive pencil (ISP) preparation

The detailed process of the ISP electrode preparation has been described in our previous publication [48]. Briefly, a zeolite and graphite powder were mixed in a 40:60 mass ratio using a ball-mill until a uniform mixture is obtained. Subsequently, the mixture was placed in a 13 mm KBr pellet die (Specac) and pressed by the hydraulic bench press applying 4 tonnes load to obtain a pellet (ISP). The electrode substrate was prepared by cutting a strip of a PET sheet (2.0 ×3.0 cm), which was then etched (aluminium oxide, grit 240). ISP was used to draw a line onto the PET sheet until the measured resistance of the electrode was less than 3 kΩ.

2.3. Potentiometric measurements

Responses of all freshly prepared, non-conditioned electrodes were recorded using the Lawson Labs Inc. 16-channel EMF-16 interface (3217 Phoenixville Pike Malvern, PA 19355, USA) in the stirred solution against a double-junction Ag/AgCl reference electrode with a 1.0 M of LiOAc bridge electrolyte (Fluka). For the measurement of the potentiometric responses, all the electrodes were immersed into 200 mL of ultrapure water followed by stepwise addition of the standards of known concentration, which were prepared using 0.1 M stock solutions of various salts (Table S1). Potentiometric responses were recorded after each addition. The electrodes were rinsed with ultra-pure water and dried before immersing into the next sample to prevent carryovers. The ion activities were calculated from the calibration curve using the Nikolsky-Eisenman equation, while the activity coefficients (log a) were calculated according to the Debye-Hückel approach. Six electrodes of the same kind were used, but for clarity reasons, the averaged responses and the standard deviations have been presented.

2.4. Data processing

All the calculations were performed using the Unscrambler 9.7 (CAMO, Norway) software. To study the influence of the zeolite type on the electrochemical response characteristics of the corresponding sensors we applied two different chemometric approaches. The first was based on principal component analysis (PCA). PCA is a common tool for exploratory data analysis that allows convenient visualisation of the initial multivariate dataset in the form of 2D plots yielding valuable information on the similarity and dissimilarity of the studied samples (in our case sensors). A detailed description of PCA methodology can be found elsewhere [49]. In the case of PCA, the analysed data matrix was comprised of the zeolite properties data set obtained for all the studied materials.

The second approach was based on partial least squares regression (PLS). To relate the values of the sensor responses towards different ions with the physical and chemical properties of the utilised zeolites, the following multivariate regression model was built:

$$\boldsymbol{Sensitivity} = \boldsymbol{b_0} + \boldsymbol{b_1}\times\boldsymbol{Property_1} + \boldsymbol{b2}\times\boldsymbol{Property_2} + \ldots + \boldsymbol{b_i}\times\boldsymbol{Property_i}.$$

The values of b_i coefficients were calculated according to the PLS algorithm [50]. The zeolite properties are listed in Table S2. The matrix of properties was mean-centred and normalised column-wise with standard deviation values for each property prior to the calculations. The obtained values of regression coefficients b_i were used to judge the effect of different properties on the sensitivity values.

3. Results and discussion

3.1. Zeolite characterisation

The range of zeolites utilised in this work includes sixteen materials, most of which are commercially available, with a significant variation of compositions and structural properties. This is important for the fabrication of inexpensive sensors as well as for generating a better prediction model for the selection of zeolites with superior performance for sensor applications.

Fig. 1 presents a typical example of characterisation data for the NaY zeolite. The XRD pattern is indicative of a highly crystalline material with the FAU structure type and the size of crystalline domain of 0.8 μm, which is in accord with the electron microscopy data. This is also confirmed by the nitrogen adsorption results: NaY possesses a 3D channel network with the pore size of just over 7 Å. The low intensity of the SiOH peak in the FTIR spectra is characteristic of a zeolite with a relatively large particle size and very few structural defects.

A complete set of characterisation results for all 16 zeolites utilised in this study is presented in the Supplementary Information section. The XRD patterns of the studied zeolites (Figs. S1-S16) correspond to those available in the literature [51], with all materials demonstrating a high degree of crystallinity. The XRD data have been also used to determine the size of the crystalline domain (Table S2), which varied from 0.9 to 0.02 μm. The chemical composition data (SEM-EDX) show a wide range of Si/Al ratios (1−40) and the content of extraframework cations. Synthetic materials contain varying concentrations of NH_4^+, Na^+ and K^+ ions, while in the natural zeolites Ca^{2+}, Mg^{2+} and Fe^{3+} are present as well (Table S2). Large-, medium- and small-pore zeolites have been utilised with the pore sizes from 3.3 to 7.5 Å. These materials possess 1D, 2D or 3D networks of channels and cages [52]. In addition, the studied zeolites demonstrate a diverse range of particle sizes (SEM or TEM measurements) and concentration of the terminal silanol groups (Si-OH) (Figs. S17-S32). The latter is expected to increase with decreasing crystal size (Table S2). All these properties can influence the interactions between the zeolite and cations in solution, leading to different selectivity and sensitivity of various zeolite-modified sensors.

In our previous work [48], the response of NaX-containing ISP--drawn electrodes to a number of cations was demonstrated as a proof of concept (Fig. 2). It was determined that the optimum composition for ISP pellets is 60–40 wt% graphite-zeolite ratio since the highest slope values are obtained. The lower zeolite content results with lower potentiometric response since there is less of the functional element present, while higher zeolite content leads to brittle pellets and the loss of drawing ability. Also, the load of 4 tonnes enables more compact pellets than 2 tonnes, while keeping the zeolite framework largely intact. Thus the contact between zeolite and graphite particles is improved. On the other hand, load of 6 tonnes leads to a decrease in potentiometric responses indicating that some framework degradation is taking place as confirmed by XRD data. The optimum response for Na^+ was 55.1 mV/decade, which is close to a Nernstian response of

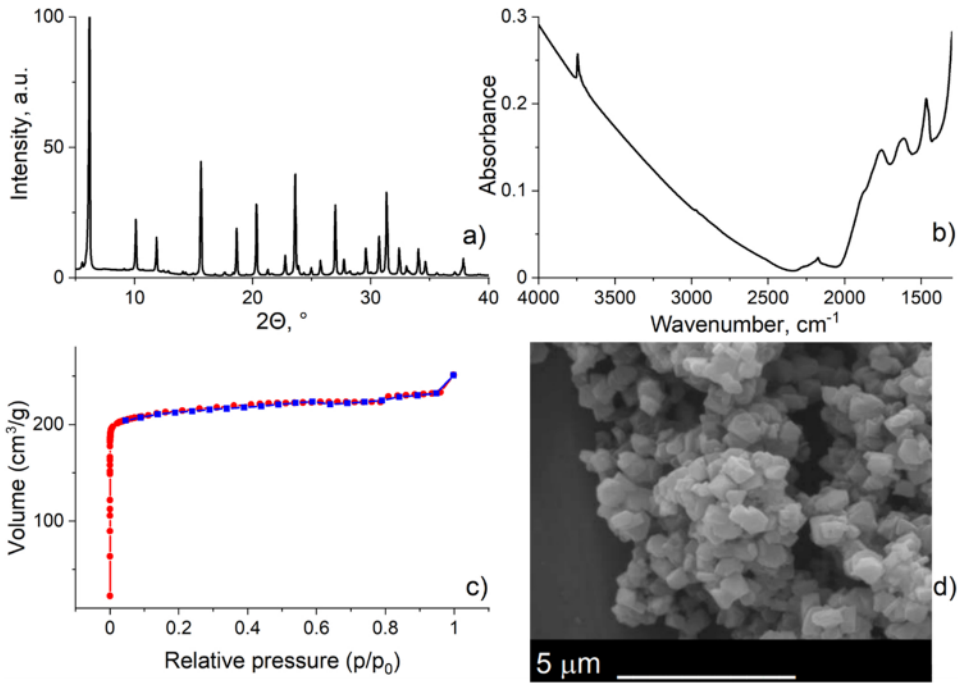

Fig. 1. Characterisation data obtained for NaY zeolite: (a) XRD pattern, (b) FTIR spectrum, (c) nitrogen adsorption-desorption isotherm, and (d) SEM micrograph.

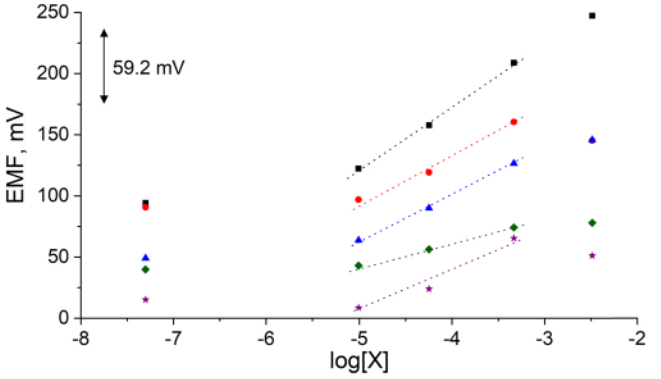

Fig. 2. Sensitivity data obtained with NaX-containing ISP-drawn electrodes for Na^+ cations (■black), K^+ (●red), NH_4^+ (▲blue), Ca^{2+} (♦green), Mg^{2+} (*purple), potentiometric responses are offset for clarity.

59.2 mV/decade. ISP-drawn electrodes were used as disposable since the loss of response is observed over prolonged exposure to water, most likely do to water ingress in the voids between particles of graphite/zeolite composite layer. Previously, for bulk "piston-type" electrodes it was attempted to overcome this problem by using fillers, such as mineral oil and paraffin [17,53]. However, even then the surface layers of such electrodes had to be removed by abrasion after several experiment cycles to regain the detection ability. Although the zeolite hydrophilicity varies with Si/Al ratio, all the zeolites used in this work (SiAl = 1–40) readily absorbed water in contact angle experiments. Therefore, the effect on the water ingress was not considered as relevant. Examples of the sensor data obtained for five cations (K^+, Na^+, NH_4^+, Ca^{2+}, Mg^{2+}) using ISP-drawn electrodes based on the slopes of calibration curves in the concentration range from 10^{-4} to 10^{-2} M are presented in Table 2. Most zeolites followed the Hoffmeister series of cations (e.g. $NH_4^+ > Cs^+ > Rb^+ > K^+ > Na^+ > Li^+ > Mg^{2+} > Ca^{2+}$), which has also been observed as a general trend for the literature values (Table 1 and references therein). In contrast, the sensitivity towards K^+ is higher than that for NH_4^+; also, K-containing zeolites have shown a high response to Ca^{2+} ions. Although many reports [13–15,43–45] have shown that the highest responses are observed for Cs^+, this cation has not been included in this study since the target application of our work is monitoring plant nutrients. The results presented demonstrate that the potentiometrically determined sensitivities deviate from the ideal Nernstian response, at the same time providing variability that can be related to the physical and chemical properties of the studied zeolites. PLS modelling has been used to relate these properties to potentiometric responses of the ISP-drawn electrodes, while PCA models have been employed to evaluate the zeolite properties data set.

Table 2
Slopes of potentiometric responses of ISP-drawn electrodes (the slopes are measured in mV/dec, in the range of log[*c*] from −5 to −3.25 using chlorides of mono- and divalent cations, and are presented as a mean of 6 measurements ± the standard deviation). Note that the range of log[*c*] was dictated by the observed linearity while the possible origin of linearity loss at log[*c*] > −3.25 is discussed in detail in Jendrlin et al [48].

Zeolite	Na^+	K^+	NH_4^+	Ca^{2+}	Mg^{2+}
NaX	55 ± 4	37 ± 5	37 ± 4	19 ± 10	35 ± 7
KX	31 ± 5	30 ± 4	34 ± 8	72 ± 5	22 ± 6
NaY	42 ± 5	70 ± 3	39 ± 3	13 ± 3	17 ± 3
KY	28 ± 3	48 ± 3	42 ± 7	53 ± 7	18 ± 2
NaA	29 ± 2	34 ± 3	14 ± 2	15 ± 2	5 ± 3
KA	23 ± 5	31 ± 2	6 ± 1	45 ± 8	-6 ± 3
MOR	47 ± 4	57 ± 5	34 ± 4	28 ± 5	12 ± 5
FER	17 ± 5	41 ± 12	27 ± 6	14 ± 2	10 ± 2
BEA 12	21 ± 5	12 ± 5	23 ± 4	30 ± 10	15 ± 8
BEA 19	30 ± 4	35 ± 3	27 ± 4	29 ± 6	8 ± 3
ZSM-5	18 ± 3	42 ± 4	20 ± 5	11 ± 3	6 ± 5
LTL	33 ± 3	58 ± 7	35 ± 3	53 ± 10	20 ± 9
MAP	14 ± 5	28 ± 5	28 ± 3	35 ± 3	15 ± 3
HEU-A	19 ± 2	46 ± 6	40 ± 2	43 ± 2	11 ± 2
HEU-B	15 ± 4	8 ± 8	12 ± 2	8 ± 6	10 ± 2
HEU-C	22 ± 3	34 ± 13	15 ± 7	25 ± 7	12 ± 2

3.2. PCA modelling

PCA modelling has been performed to visualise the variability of zeolite properties. (Fig. 3) The following parameters have been used for

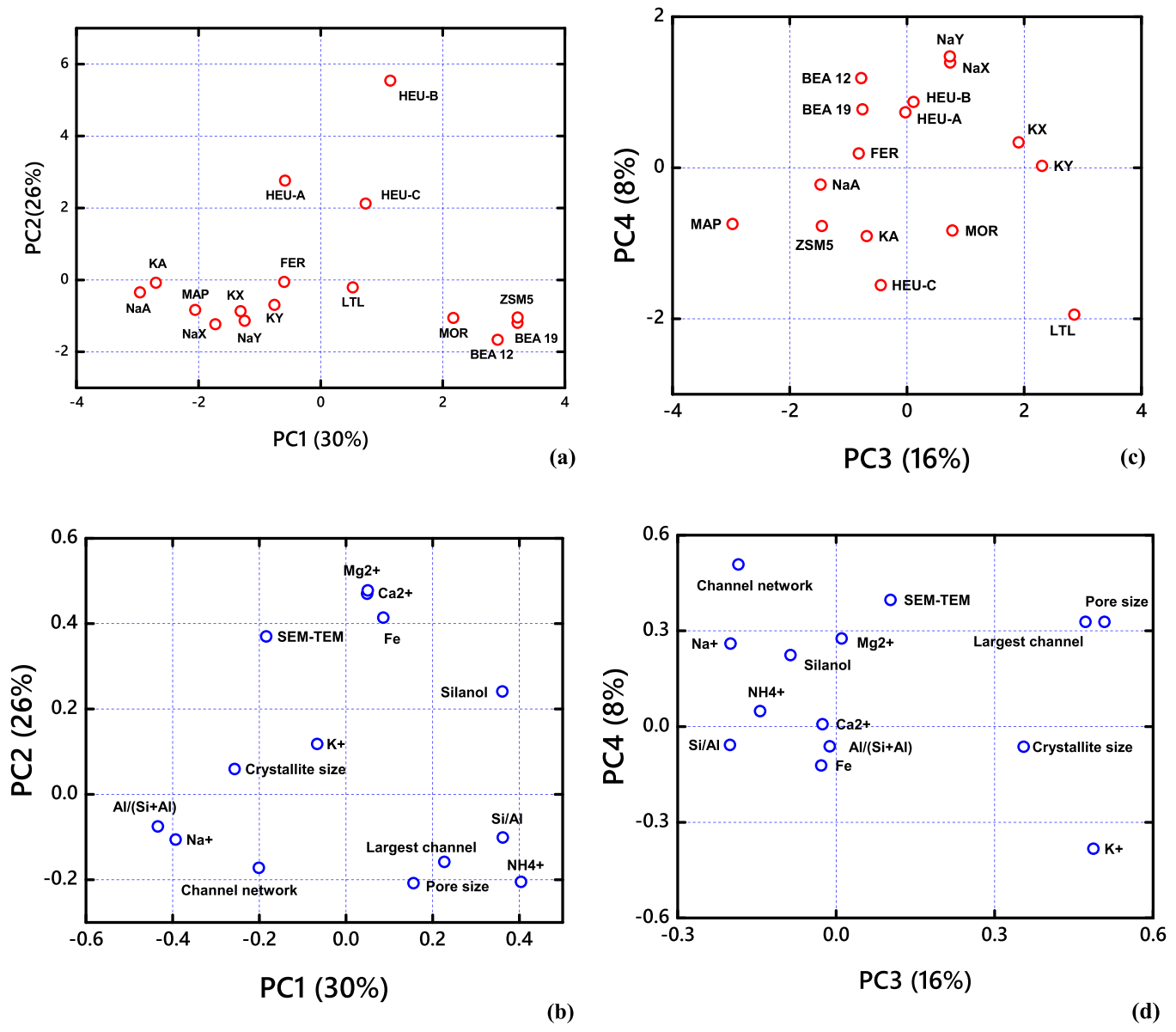

Fig. 3. PCA score plot based on the properties of the zeolites PC1-PC2 (a), PCA loadings plot for PC1-PC2 (b), PCA score plot based on the properties of the zeolites PC3-PC4 (c), and PCA loadings plot for PC3-PC4 (d).

the studied zeolites: Si/Al; Al/(Si+Al); Pore Size (Å); Largest Channel, MR; Channel Network; Extraframework Cations (Na^+, K^+, NH_4^+, Ca^{2+}, Mg^{2+} or Fe^{3+}); Crystallite Size (XRD); Particle Size (SEM-TEM); SiOH Intensity (Table S2).

PCA score plots are the so-called maps of samples, where each point represents one zeolite. The location of the points in the PC space indicates their similarity or dissimilarity in terms of the variables employed for the calculation of PCs (here, these are the characteristics of zeolites). The points located close to each other are similar, and vice versa. A PCA loadings plot is a "map of variables". It shows the importance of a particular variable for the direction of PC. Each point represents one zeolite parameter. If the variables are close to each other in the loadings plot, they are positively correlated. If they are located opposite to each other relative to the graph origin, they are negatively correlated. The percentage variance is the amount of variability in the data taken into account by each PC. Thus, for PC1-PC2 space, where the explained variance is 56%, the Pore Size and Largest Channel variables are positively correlated, whereas the presence of Na^+ and that of NH_4^+ as extraframework cations are negatively correlated. It can also be observed that zeolites with the lower Al content (MOR, BEA-12, BEA-19, ZSM-5) are grouped opposite to zeolites with the higher Al content, such as NaX, NaY, NaA, KX, KY, KA. For example, it can be deduced from the PC1-PC2 plot that NaA is different from ZSM-5 largely due to the Pore Size, Al/(Si+Al), Na^+, NH_4^+ and Si/Al parameters (this conclusion is made considering both scores and loadings together), which agrees with their structural characterisation data, catalytic performance and spectroscopic analyses.

For the PC3-PC4 space, the explained variance is 24%, the parameters Pore Size and Largest Channel variables are positively correlated, similar to the PC1-PC2 plot. On the other hand, Crystallite Size and Silanol Intensity are negatively correlated, as are the presence of Na^+ and K^+ extraframework cations. It can also be observed that zeolites with larger pore size, i.e. NaX, NaY, KX, KY, are grouped opposite of zeolites with a smaller pore size such as NaA, KA or MAP. For example, it can be concluded from the PC3-PC4 plot that zeolite MAP is different from LTL mainly due to the Channel Network, Silanol Intensity, SEM-TEM, Na^+, K^+ and Si/Al parameters (this conclusion is made considering both scores and loadings together). Once again, this is in

accordance with the characterisation data available for these materials.

Overall, these data confirm that the zeolites utilised in this work for the fabrication of ISPs demonstrate a significant variation of compositions and structural properties, which is important for a more reliable PLS modelling.

3.3. PLS modelling

Multivariate regression models have been constructed to identify the most important properties of zeolites that impact the sensitivity of potentiometric sensors. The set of parameters for all zeolites has been related to the potentiometric sensitivity towards a particular ion (K^+, NH_4^+, Na^+, Ca^{2+}, Mg^{2+}). Since all parameters are in different units, their values have been autoscaled prior to modelling. The figures below are presented as "measured vs predicted" plots indicating real sensitivity values towards an ion (in mV/dec) and those predicted by the PLS model during calibration and cross-validation. The absolute values of the regression coefficients in the corresponding charts indicate the importance of particular zeolite parameters in the development of sensor response.

For zeolites as electroactive components to have an electrochemical response, a prerequisite requirement is that a cation can enter the zeolite channel network. If the zeolite pores are too small for solvated cations to enter, no or almost no electrochemical response is observed [16,33,34]. Based on their pore size, all the utilised zeolites could accommodate the studied cations, Table S2, although the number of cations entering the zeolite pores would depend on the Si/Al ratio and specific structural features of the zeolite. It should be noted that the term "cation size" should be used with caution, as it is the size of the hydrated cations that is important, and indeed, this can explain the high responses for Cs^+ reported in the literature. At the same time, the degree of hydration of different cations inside the zeolite pores is not well defined and can change depending on the zeolite and the experimental conditions. Fig. 4**a** presents a PLS model predicting the sensor sensitivity towards NH_4^+ based on a number of zeolite characteristics. The model demonstrates that all the natural zeolites (HEU-A, HEU-B, HEU-C) and zeolite MAP are outliers. This can be explained by the less uniform structure and composition of natural zeolites as compared to the synthetic counterparts, which could cause the potentiometric responses to vary from the rest of the zeolites. On the other hand, zeolite MAP is known for its flexible structure, indeed, the unit cell volume can change by up to 30% upon hydration-dehydration [54], which may have an impact on its ion-exchange properties. Therefore, HEU-A, HEU-B, HEU-C and MAP have been excluded from the initial model, leading to a significantly better regression model (Fig. 4**b**, Table 3). This limits the predictions to the commercially available samples only, which is associated with their better defined characteristics. We believe that the exclusion of HEU and MAP zeolites should not hinder the applicability of the proposed model.

The regression coefficients of this model (Fig. 4**c**) indicate that in addition to Pore Size and Largest Channel, previously recognised as important parameters [26,33,34], relevant parameters contributing to this model are Al/(Si+Al) and Silanol Intensity. The former is linked to the Si/Al ratio but is a better measure of the Al concentration, which affects the total ion-exchange capacity of a zeolite, while the latter is related to the particle size as smaller particles have a higher external surface area covered by silanols. These results may be linked to a better dispersion of the smaller zeolite particles in the graphite matrix. In addition, as the ion-exchange process is limited by the diffusion of cations into zeolite channels, the mass-transfer limitations could become important for zeolites with a very different particle size. However, based on independent experiments, e.g. ion-exchange studies, and considering the time scale of the experiments, we believe our measurements have been conducted under steady-state conditions. However in general, cation diffusion in small and large zeolite crystals may have an effect on the sensitivity of ISP-drawn electrodes towards species of interest.

A PLS regression model "measured vs predicted" for the

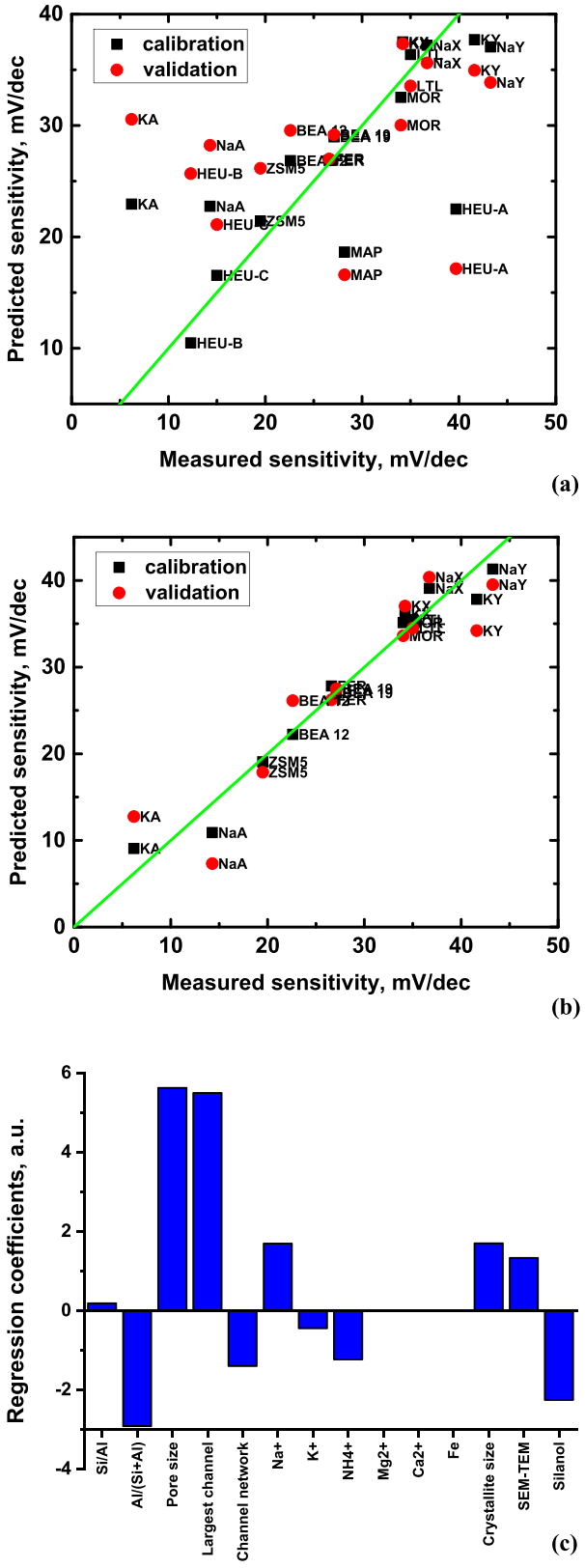

Fig. 4. PLS regression model for the potentiometric sensitivity towards NH_4^+, (a) including all zeolites, (b) without MAP and HEU zeolites (RMSEC 2.1 mV/dec, RMSECV 4.1 mV/dec, R^2cal 0.96, R^2val 0.88), and (c) regression coefficients for the PLS regression model with 4 LVs for the potentiometric sensitivity towards NH_4^+, which excludes HEU and MAP zeolites.

Table 3
PLS regression data for all the calculated systems.

Model cation	RMSEC	RMSECV	R^2-cal	R^2-val
NH_4^{+} (*)	2.1	4.1	0.96	0.88
Ca^{2+} (*)	7.41	12.3	0.84	0.64
Mg^{2+} (*)	4.2	7.8	0.81	0.46
K^{+}	4.2	9.0	0.90	0.59
Na^{+} (**)	2.1	6.0	0.94	0.52

(*) without HEUs and MAP
(**) without ZSM-5.

potentiometric sensitivity for Ca^{2+} is shown in Fig. 5**a** alongside the bar chart with the regression coefficients presented in Fig. 5**b** (with three natural zeolites and zeolite MAP excluded from the model).

Parameters affecting the Ca^{2+} regression plot (Fig. 5**b**) the most are the presence of sodium and potassium as extraframework cations and the aluminium content in zeolites, which is described by the Si/Al ratio and the Al fraction. In contrast to the NH_4^{+} sensitivity model, the presence of K^{+} and Na^{+} are the most significant contributors. This feature has not been observed previously for other electrochemical techniques (cyclic voltammetry and indirect amperometry) as a relevant parameter. Indirectly, the potentiometric sensitivity can be enhanced by preconcentration of solutions containing the same kind of cations [43–45], but the effect of extraframework cations present in a zeolite on the PLS regression model for the potentiometric response has not been reported. Si/Al ratio has been recognised as an important parameter in agreement with the general ion-exchange observations that the zeolites with a higher Al content have a greater affinity to multivalent cations, while the more siliceous zeolites have a greater affinity towards monovalent cations [1].

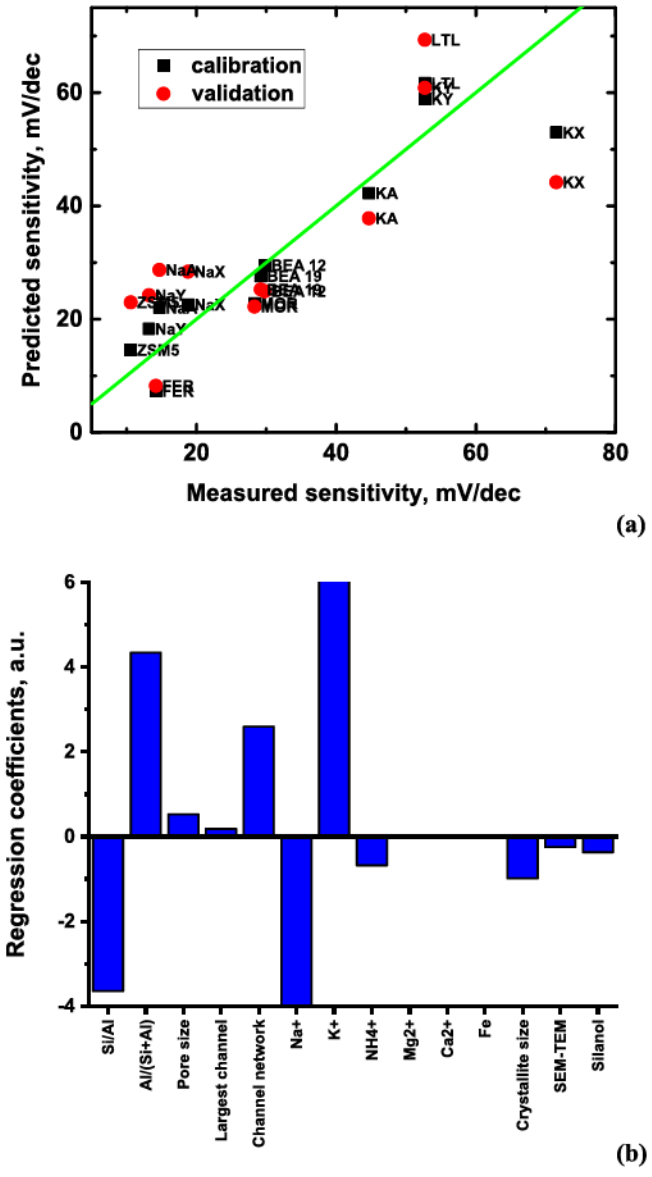

Fig. 5. PLS regression model for the potentiometric sensitivity towards Ca^{2+} without MAP and HEU zeolites, (RMSEC 7.4 mV/dec, RMSECV 12.3 mV/dec, R^2cal 0.84, R^2val 0.64), b) PLS regression coefficients for the model with 3 LVs (b).

The PLS regression model parameters for all studied cations (NH_4^{+}, K^{+}, Na^{+}, Ca^{2+} and Mg^{2+}) are compiled in Table 3. In general, these data (in particular, RMSECV values, which are given in mV/dec) imply that semi-quantitative models for the prediction of zeolite sensor sensitivity can be constructed using PLS regression. The parameters of the models assume that the best correlation is observed for ammonium and calcium.

During the initial characterisation of the ISP-drawn electrodes, the sensitivities towards several transition metal cations have been recorded [48]. However, the responses towards these cations have been very low and inconsistent, and therefore no viable models have been established. These findings can be linked to the complex nature of the ion-exchange processes involving transition metal ions, which are frequently accompanied by the precipitation on the external surface of zeolites [1].

It should be noted that in our previous work [48], PLS modelling was used to predict the concentration of Mg^{2+} (10^{-4}-10^{-2} M) in mixture solutions of 4 cations (K^{+}, NH_4^{+}, Ca^{2+}, Mg^{2+}). A total of 20 plant nutrient model water solutions were prepared according to the experimental design for multivariate calibration. The cross-validation R^2 coefficient was 0.83 and RMSECV 0.34 log[Mg^{2+}]. Also, the model was used to predict the concentration of Mg^{2+} in a test set with 6 randomly removed values. The Pearson's R was 0.944 and the mean relative error 8.4%.

Using the data obtained so far, good quality models for the commercially available synthetic zeolites have been generated; however, they can be further improved by including a greater number of samples used for calibration. Additionally, potentiometric responses for a variety of natural zeolites are required, either to enhance the performance of the existing models containing both synthetic and natural zeolites or to establish a new model specifically for natural zeolite.

4. Conclusions

In this work, the potentiometric response of ISP-drawn zeolite-modified electrodes, containing thirteen synthetic and three natural zeolites, in aqueous solutions of Na^{+}, K^{+}, NH_4^{+}, Ca^{2+} and Mg^{2+} is related to a range of zeolite characteristics using PCA and PLS modelling. It is concluded that physical properties impact the zeolite-modified potentiometric sensor performance. In addition to the previously stated steric factors, such as pore size, the important features, which by and large determine the sensor performance, are the Si/Al ratio and the presence of specific extraframework cations. For example, K^{+} and Na^{+} affect the potentiometric sensitivity towards Ca^{2+}. The level of precision attained by the models implies that semi-quantitative predictions are possible. To improve the computational models further, a larger dataset with a wider range of zeolite-modified sensors is needed. The constituent materials of such sensors should have a set of well-defined properties, which can be designed and tuned for a particular application. It can be expected that synthetic rather than natural zeolites would satisfy such requirements. Indeed, although the latter are less expensive and are available in large quantities, it is challenging to control their properties. It should be noted that the selectivities of single zeolite-modified potentiometric sensors are limited, especially as compared to the traditional ion-selective electrodes. Therefore, incorporating them into multi-sensor arrays is required to optimise the operation of such sensors.

This should ultimately lead to the improvement of multi-sensor array performance, both in terms of sensitivity and selectivity, in a range of analytical applications, including among many others agriculture, environmental monitoring and food science.

CRediT authorship contribution statement

Martin Jendrlin: Validation, Formal analysis, Investigation, Data curation, Writing – original draft, Writing – review & editing. **Dmitry Kirsanov**: Conceptualization, Methodology, Validation, Formal analysis, Investigation, Data curation, Writing – original draft, Writing – review & editing, Visualization. **Vladimir Zholobenko**: Conceptualization, Methodology, Validation, Formal analysis, Investigation, Data curation, Writing – original draft, Writing – review & editing, Visualization. **Aleksandar Radu**: Conceptualization, Methodology, Formal analysis, Resources, Writing – original draft, Writing – review & editing, Supervision, Project administration, Funding acquisition.

Declaration of Competing Interest

The authors declare that they have no known competing financial interests or personal relationships that could have appeared to influence the work reported in this paper.

Acknowledgements

This work was supported by the Royal Society (IES\R3\203138), NSF-UKRI (grant NE/T012331/1), and Keele University. The authors are grateful to Zeodex, UK, and Prof A. Walcarius (Université de Lorraine, France) for their generous provision of heulandite samples.

Appendix A. Supporting information

Supplementary data associated with this article can be found in the online version at doi:10.1016/j.snb.2021.131343.

References

[1] Introduction to Zeolite Science and Practice, Elsevier Science, 2007.
[2] X. Xu, J. Wang, Y. Long, Zeolite-based materials for gas sensors, Sensors 6 (2006) 1751–1764.
[3] Y. Zheng, X. Li, P.K. Dutta, Exploitation of unique properties of zeolites in the development of gas sensors, Sensors 12 (2012) 5170–5194.
[4] K. Sahner, G. Hagen, D. Schönauer, S. Reiß, R. Moos, Zeolites - versatile materials for gas sensors, Solid State Ion. 179 (2008) 2416–2423.
[5] S.N. Talapaneni, J. Grand, S. Thomas, H.A. Ahmad, S. Mintova, Nanosized Sn-MFI zeolite for selective detection of exhaust gases, Mater. Des. 99 (2016) 574–580.
[6] P. Yang, et al., Design of efficient zeolite sensor materials for n-hexane, Anal. Chem. 79 (2007) 1425–1432.
[7] A. Walcarius, Zeolite-modified electrodes in electroanalytical chemistry, Anal. Chim. Acta 384 (1999) 1–16.
[8] A. Walcarius, Electroanalytical applications of microporous zeolites and mesoporous (organo)silicas: recent trends, Electroanalysis 20 (2008) 711–738.
[9] D.R. Rolison, Zeolite-modified electrodes and electrode-modified zeolites, Chem. Rev. 90 (1990) 867–878.
[10] J.C. Jansen, M. Stocker, H.G. Karge, J. Weitkamp, Advanced Zeolite Science and Applications, Elsevier, 1994.
[11] R.A. Durst, A.J. Bäumner, R.W. Murray, R.P. Buck, C.P. Andrieux, Chemically modified electrodes: recommended terminology and definitions, Pure Appl. Chem. 69 (1997) 1317–1323.
[12] A. Walcarius, V. Ganesan, O. Larlus, V. Valtchev, Low temperature synthesis of zeolite films on glassy carbon: towards designing molecularly selective electrochemical devices, Electroanalysis 16 (2004) 1550–1554.
[13] N.P. Evmiridis, M.A. Demertzis, A.G. Vlessidis, Effect of treatment of synthetic zeolite-polymer membranes on their electrochemical-potential response characteristics, Fresenius J. Anal. Chem. 340 (1991) 145–152.
[14] G. Johansson, L. Risinger, A cesium-selective electrode prepared from a crystalline synthetic zeolite of the mordenite type, Anal. Chim. Acta 119 (1980) 25–32.
[15] S. Matysik, F.M. Matysik, J. Mattusch, W.D. Einicke, Application of zeolite-polydimethylsiloxane electrodes to potentiometric studies of cationic species, Electroanalysis 10 (1998) 98–102.
[16] R.M. Barrer, S.D. James, Electrochemistry of crystal-polymer membranes. Part II. Membrane potentials, J. Phys. Chem. 64 (1960) 421–427.
[17] A. Walcarius, Zeolite-modified paraffin-impregnated graphite electrode, J. Solid State Electrochem. 10 (2006) 469–478.
[18] A. Walcarius, V. Vromman, J. Bessiere, Flow injection indirect amperometric detection of ammonium ions using a clinoptilolite-modified electrode, Sens. Actuators B Chem. 56 (1999) 136–143.
[19] J. Wang, A. Walcarius, Zeolite-modified carbon paste electrode for selective monitoring of dopamine, J. Electroanal. Chem. 407 (1996) 183–187.
[20] C.E. Marshall, The use of zeolitic membrane electrodes (1939).
[21] S. Sohrabnejad, M.A. Zanjanchi, M. Arvand, M.F. Mousavi, Evaluation of a PVC-based thionine-zeolite and zeolite free membranes as sensing elements in ion selective electrode, Electroanalysis 16 (2004) 1033–1037.
[22] E.M. Maximiano, F. de Lima, C.A.L. Cardoso, G.J. Arruda, Modification of carbon paste electrodes with recrystallized zeolite for simultaneous quantification of thiram and carbendazim in food samples and an agricultural formulation, Electrochim. Acta 259 (2018) 66–76.
[23] S.N. Azizi, S. Ghasemi, F. Amiripour, Nickel/P nanozeolite modified electrode: a new sensor for the detection of formaldehyde, Sens. Actuators B Chem. 227 (2016) 1–10.
[24] H.S. Hashemi, A. Nezamzadeh-Ejhieh, M. Karimi-Shamsabadi, A novel cysteine sensor based on modification of carbon paste electrode by Fe(II)-exchanged zeolite X nanoparticles, Mater. Sci. Eng. C 58 (2016) 286–293.
[25] A. Nezamzadeh-Ejhieh, H.S. Hashemi, Voltammetric determination of cysteine using carbon paste electrode modified with Co(II)-Y zeolite, Talanta 88 (2012) 201–208.
[26] M.D. Baker, C. Senaratne, J. Zhang, Effects of supporting electrolyte and zeolite Co-cations on the electrochemical response of zeolite-modified electrodes, J. Chem. Soc. Faraday Trans. 88 (1992) 3187–3192.
[27] A. Walcarius, L. Lumberts, E.G. Derouane, Cation determination in aqueous solution using the methyl viologen-doped zeolite-modified carbon paste electrode, Electroanalysis 7 (1995) 120–128.
[28] S. Kilinc Alpat, U. Yuksel, H. Akcay, Development of a novel carbon paste electrode containing a natural zeolite for the voltammetric determination of copper, Electrochem. Commun. 7 (2005) 130–134.
[29] A. Nezamzadeh-Ejhieh, A. Badri, Surfactant modified ZSM-5 zeolite as an active component of membrane electrode towards thiocyanate, Desalination 281 (2011) 248–256.
[30] M. Hasheminejad, A. Nezamzadeh-Ejhieh, A novel citrate selective electrode based on surfactant modified nano-clinoptilolite, Food Chem. 172 (2015) 794–801.
[31] L.R. Siara, F. De Lima, C.A.L. Cardoso, G.J. Arruda, Electrochemically pretreated zeolite-modified carbon-paste electrodes for determination of linuron in an agricultural formulation and water, Electrochim. Acta 151 (2015) 609–618.
[32] J. Dong, X. Zhou, H. Zhao, J. Xu, Y. Sun, Reagentless amperometric glucose biosensor based on the immobilization of glucose oxidase on a ferrocene@NaY zeolite composite, Microchim. Acta 174 (2011) 281–288.
[33] A. Walcarius, T. Barbaise, J. Bessiere, Factors affecting the analytical applications of zeolite-modified electrodes preconcentration of electroactive species, Anal. Chim. Acta 340 (1997) 61–76.
[34] A. Walcarius, Factors affecting the analytical applications of zeolite modified electrodes: indirect detection of nonelectroactive cations, Anal. Chim. Acta 388 (1999) 79–91.
[35] D. Kirsanov, et al., A pencil-drawn electronic tongue for environmental applications, Sensors 21 (2021) 4471.
[36] D.R. Rolison, R.J. Nowak, T.A. Welsh, C.G. Murray, Analytical implications of zeolites in overlayers at electrodes, Talanta 38 (1991) 27–35.
[37] J.P. Li, T.Z. Peng, C. Fang, Screen-printable sol-gel ceramic carbon composite pH sensor with a receptor zeolite, Anal. Chim. Acta 455 (2002) 53–60.
[38] K. Yu, et al., Electrosynthesized polypyrrole/zeolite composites as solid contact in potassium ion-selective electrode, Electrochim. Acta 228 (2017) 66–75.
[39] S. Senthilkumar, A.J. King, S.M. Holmes, R.A.W. Dryfe, R. Saraswathi, Potentiometric sensing of heavy metal ions using a novel zeolite Y membrane, Electroanalysis 18 (2006) 2297–2304.
[40] M.L. Hamlaoui, R. Kherrat, M. Marrakchi, N. Jaffrezic-Renault, A. Walcarius, Development of an ammonium ISFET sensor with a polymeric membrane including zeolite, Mater. Sci. Eng. C 21 (2002) 25–28.
[41] M.L. Hamlaoui, et al., Development of a urea biosensor based on a polymeric membrane including zeolite, Anal. Chim. Acta 466 (2002) 39–45.
[42] A.J. King, G.C. Lillie, V.W.Y. Cheung, S.M. Holmes, R.A.W. Dryfe, Potentiometry in aqueous solutions using zeolite films, Analyst 129 (2004) 157–160.
[43] M. Arvand-Barmchi, M.F. Mousavi, M.A. Zanjanchi, M. Shamsipur, A PTEV-based zeolite membrane potentiometric sensor for cesium ion, Sens. Actuators B Chem. 96 (2003) 560–564.
[44] M. Arvand, M. Moghimi, M.A. Bagherinia, Zeolite-modified sol-gel electrode as an electrochemical sensor for potentiometric determination of cesium ions in water samples, Anal. Lett. 42 (2009) 393–408.
[45] M. Giahi, H. Aghaie, M. Arvand, A.M. Hejri, Application of a zeolite-poly(vinyl chloride) electrode to potentiometric studies of alkali metal ions, Russ. J. Electrochem. 41 (2005) 1290–1295.
[46] A. Al-Ani, R.J. Darton, S. Sneddon, V. Zholobenko, Nanostructured zeolites: the introduction of intracrystalline mesoporosity in basic faujasite-type catalysts, ACS Appl. Nano Mater. 1 (2017) 310–318.
[47] V. Zholobenko, et al., Probing the acid sites of zeolites with pyridine: quantitative AGIR measurements of the molar absorption coefficients, J. Catal. 385 (2020) 52–60.
[48] M. Jendrlin, et al., Ion sensing pencil: draw your own sensor, Sens. Actuators B Chem. 337 (2021), 129751.

[49] Q. Wang, Q. Gao, X. Gao, F. Nie, Angle principal component analysis, in: Angle Principal Component Analysis, 2017, pp. 2936–2942.
[50] S. Wold, M. Sjöström, L. Eriksson, PLS-regression: a basic tool of chemometrics, in: Chemometrics and Intelligent Laboratory Systems, 58, Elsevier, 2001, pp. 109–130.
[51] M.M.J. Treacy, J.B. Higgins, Collection of Simulated XRD Powder Patterns for Zeolites Fifth (5th) Revised Edition, 2007. doi:10.1016/B978-0-444-53067-7.X5470-7.
[52] C. Baerlocher, L.B. Mccusker, D.H. Olson, Atlas of Zeolite Framework Types, Elsevier, 2007.
[53] J. Wang, A. Walcarius, Zeolite containing oxidase-based carbon paste biosensors, J. Electroanal. Chem. 404 (1996) 237–242.
[54] V.L. Zholobenko, et al., Structural transitions in zeolite P an in situ FTIR study, J. Chem. Soc. Faraday Trans. 94 (1998) 1779–1781.

Martin Jendrlin obtained his M.Sc. at the University of Zagreb, Croatia (2017) and is currently a Ph.D. student at Keele University, UK. His research interests focus on synthesis of zeolites and their application in electrochemical sensors.

Aleksandar Radu obtained Ph.D. in analytical chemistry from Auburn University, USA in 2005. He is currently senior lecturer at Keele University, UK. His research interests are in utilisation of advanced materials for the development of chemical sensors and analytical methodologies for application in bio/environmental analysis.

Vladimir Zholobenko obtained his Ph.D. in chemistry at Moscow State University in 1990. He is currently a senior lecturer in the School of Chemical and Physical Sciences at Keele University. His research activities are at the interface of materials science and physical chemistry, catalysis and analytical sciences, spectroscopic characterisation techniques and environmental applications of nanostructured materials.

Dmitry Kirsanov received his Ph.D. in analytical chemistry at Saint-Petersburg State University in 2005. Currently, he is working as a professor at the Institute of Chemistry of Saint-Petersburg University. His main research interests involve electrochemical and optical multisensor systems and multivariate data processing(chemometrics).